Journal of the American College of Cardiology
© 2006 by the American College of Cardiology Foundation
Published by Elsevier Inc.

Vol. 47, No. 1, 2006
ISSN 0735-1097/06/$32.00
doi:10.1016/j.jacc.2005.09.008

Effects of Primary Angioplasty for Acute Myocardial Infarction on Early and Late Infarct Size and Left Ventricular Wall Characteristics

Timo Baks, MD,*† Robert-Jan van Geuns, MD, PHD,*† Elena Biagini, MD,* Piotr Wielopolski, PHD,† Nico R. Mollet, MD,*† Filippo Cademartiri, MD, PHD,*† Willem J. van der Giessen, MD, PHD,* Gabriel P. Krestin, MD, PHD,† Patrick W. Serruys, MD, PHD, FACC,* Dirk J. Duncker, MD, PHD,* Pim J. de Feyter, MD, PHD, FACC*†

Rotterdam, the Netherlands

OBJECTIVES We aimed to study the effects of early successful primary angioplasty for ST-segment elevation acute myocardial infarction (AMI) on early and late infarct size and left ventricular (LV) wall characteristics.

BACKGROUND Early reperfusion treatment for AMI preserves LV function, but the effects on early and late infarct size, end-diastolic wall thickness (EDWT), and segmental wall thickening (SWT) are not well known.

METHODS In 22 patients with successful primary angioplasty for first AMI, cine–magnetic resonance imaging (MRI), first-pass perfusion, and delayed-enhancement imaging was performed at five days and five months. The extent of microvascular obstruction (MO) was evaluated on perfusion images. Infarct shrinkage was defined as the difference between the volume of delayed-enhancement at five days and five months. The EDWT and SWT were quantified on cine-MRI.

RESULTS Infarct shrinkage occurred to the same extent in small and large infarctions [$r = 0.92$; $p < 0.001$], with a mean decrease of 31% (35 ± 21 g to 24 ± 17 g). Dysfunctional segments without MO had an increased EDWT at five days compared with remote myocardium (9.2 ± 1.7 mm vs. 8.4 ± 1.7 mm; $p < 0.001$). At five months, EDWT in these segments became comparable to the thickness of remote myocardium (7.8 ± 1.6 mm vs. 7.6 ± 1.4 mm; $p = 0.60$), and SWT improved (21 ± 15% to 40 ± 24%; $p < 0.001$) but remained impaired (40 ± 24% vs. 71 ± 29%; $p < 0.001$). Segments with MO demonstrated wall thinning at five months (6.4 ± 1.3 mm vs. 7.6 ± 1.4 mm; $p = 0.006$) and no significant recovery in SWT (12 ± 14% to 17 ± 20%; $p = 0.15$).

CONCLUSIONS Infarct size decreased by 31%. Segments without MO had early increased wall thickness and late partial functional recovery. Segments with MO showed late wall thinning and no functional recovery at five months. (J Am Coll Cardiol 2006;47:40–4) © 2006 by the American College of Cardiology Foundation

Early restoration of epicardial coronary blood flow reduces infarct size in patients with acute myocardial infarction (AMI) and has a beneficial effect on post-infarction myocardial infarct healing and left ventricular (LV) remodeling (1–3). Early reperfusion, however, might also lead to endothelial dysfunction and extravasation of fluids to the interstitium (4). Understanding the natural course of infarct healing and the effect of early reperfusion on ischemic myocardium might contribute to understanding and developing new therapies for ischemic heart disease. Recently, it was shown that contrast-enhanced magnetic resonance imaging (ce-MRI) allows the assessment of myocardial perfusion, infarct size, and LV wall thickness/function with good reproducibility and excellent correlation with histology in animal models of acute and chronic myocardial infarction (5–11). Therefore, we performed ce-MRI in patients who suffered AMI and were treated within six hours with successful drug-eluting stent implantation to study the effects on early and late infarct size and LV wall characteristics.

METHODS

Patient population. We studied 30 patients (25 men, age 53 ± 10 years) admitted to the coronary care unit with first AMI. Patient characteristics are listed in Table 1. Diagnosis was on the basis of clinical symptoms, ST-segment elevation on electrocardiogram, and angiographically demonstrated occlusion of a coronary artery. All vessels were stented with a drug-eluting stent within 6 h (mean 2.5 h) of onset of symptoms, resulting in Thrombolysis In Myocardial Infarction flow grade 3 (12). Exclusion criteria consisted of any contraindication to MRI. All participants gave written informed consent to the study protocol, which was approved by the medical ethics committee of the Erasmus

From the *Department of Cardiology, Thoraxcenter, and the †Department of Radiology, Erasmus Medical Center, University Medical Center, Rotterdam, the Netherlands.

Manuscript received March 20, 2005; revised manuscript received June 1, 2005, accepted July 27, 2005.

Abbreviations and Acronyms

AMI = acute myocardial infarction
ce-MRI = contrast-enhanced magnetic resonance imaging
EDWT = end-diastolic wall thickness
ESWT = end-systolic wall thickness
FOV = field of view
LV = left ventricle/ventricular
MO = microvascular obstruction
SWT = segmental wall thickening
TE = time to echo
TR = repetition time

Medical Center Rotterdam. The study population consisted of 22 patients who had the first MRI scan 5 ± 3 days after admission and the second MRI scan 20 ± 7 weeks later. Eight patients did not undergo a second scan: one patient died (noncardiac death), two patients had a defibrillator implanted, and five patients refused to come back. Angiographic follow-up was performed in eight patients (36%), and no in-stent restenosis was seen. In the other patients, there was no clinical evidence of recurrent myocardial ischemia, and all patients received a drug-eluting stent in the infarct-related coronary artery, with very low numbers of restenosis reported (13).

MRI protocol. A clinical 1.5-T MRI with a dedicated cardiac four-element phased-array receiver coil was used for imaging (Signa CV/i, GE Medical Systems, Milwaukee, Wisconsin). Baseline and follow-up ce-MRI protocol consisted of cine-MRI, first-pass perfusion, and delayed enhancement imaging. The cine-MRI was performed with a steady-state free-precession technique (FIESTA, GE Medical Systems) with the following imaging parameters: 24 temporal phases per slice, field of view (FOV) 32 to 36 cm × 32 to 36 cm; rectangular FOV 0.75; repetition time (TR) 3.2 to 3.7; time to echo (TE) 1.4; flip angle 45°; matrix 160 × 128, bandwidth 83 kHz, number of averages 0.75. To cover the entire LV, 9 to 12 consecutive slices of 8 mm were planned in short-axis view (gap of 2 mm) on the horizontal long axis (four-chamber view) of the LV. First-pass perfusion imaging was performed during 30 to 40 consecutive heartbeats immediately after administration of gadolinium-diethylenetriamine penta-acetic acid (DTPA) (0.1 mmol/kg; Magnevist, Schering, Germany; 4 ml/s in an antecubital vein, followed by 15 ml of saline at 4 ml/s). A special pre-saturation scheme with a notched excitation followed by a segmented gradient-echo/echo-planar readout was used (14) with the following imaging parameters: FOV 32 to 36 cm × 32 to 36 cm, rectangular FOV 0.75, TR 6.8, inversion time 150 to 175 ms, saturation pulse 90°, TE 1.2, echo train length 4, number of averages 0.75, bandwidth 125 kHz, flip angle 20°, matrix 128 × 96, slice thickness 8 mm. The temporal resolution per slice of 120 ms allowed imaging of five to eight slices per RR interval (maximum heart rate of 90 beats/min). Perfusion images were planned to cover the basal, mid, and apical part of the LV in the same orientation as the cine images. Delayed enhancement imaging was performed with a two-dimensional T1-weighted inversion-recovery gradient-echo sequence 10 to 20 min after perfusion imaging with the following parameters: FOV 32 to 36 cm × 32 to 36 cm, rectangular FOV 0.75; slice thickness 8 mm, gap 2 mm, TR 7.3, TE 1.6, flip angle 20°, inversion pulse of 180°, matrix 256 × 192, number of averages 1, bandwidth 17.9 kHz, inversion time 180 to 275 ms (adjusted per patient to null the signal of remote myocardium). Slice locations of the delayed enhancement images were copied from the cine images.

Table 1. Patient Characteristics (n = 22)

Age (yrs)	52 ± 12
Men	16 (73)
Smoking	15 (68)
Diabetes mellitus	1 (5)
Hypertension	6 (27)
Hypercholesterolemia	5 (23)
Family history of coronary artery disease	12 (55)
Creatine kinase peak (IU)	3,112 ± 2,001
Anterior infarction	15 (68)
Inferior/lateral infarction	7 (32)
Abciximab peri-procedural	14 (64)
ACE inhibitor baseline/follow-up	1 (5)/18 (82)
Beta-blocker baseline/follow-up	3 (14)/22 (100)
Clopidogrel	22 (100)
Statin follow-up	20 (91)
ASA follow-up	22 (100)
Ejection fraction 5 days (%)	48 ± 11
Ejection fraction 5 months (%)	55 ± 9

Values are presented as (%) or mean ± SD.
ACE = angiotensin-converting enzyme; ASA = acetylsalicylic acid.

Definitions and data analysis. Cine, perfusion, and delayed enhancement images were all matched for position with anatomical landmarks like papillary muscles and the insertion of the right ventricle. To quantify end-diastolic wall thickness (EDWT), end-systolic wall thickness (ESWT), LV volumes, and LV mass, epicardial and endocardial contours were detected automatically and corrected manually on short-axis cine-MRI images in 16 myocardial segments per patient with the centerline method (Mass; Medis, Leiden, the Netherlands). Segmental wall thickening (SWT) was calculated by: (ESWT − EDWT)/EDWT × 100. Myocardial segments were considered dysfunctional if SWT was 45% or less (15). Myocardial perfusion was evaluated qualitatively on first-pass perfusion images and scored as: 1 = no microvascular obstruction (MO) (homogeneous enhancement of myocardium), 2 = presence of MO (hypoenhanced region). No perfusion study had to be excluded from the analysis owing to lack of image quality. Infarcted myocardium was clearly differentiated from remote myocardium with a delayed enhancement inversion-recovery pulse sequence. Infarct size was quantified by manually tracing the delayed enhanced regions from the consecutive two-dimensional slices encompassing the LV. Delayed enhancement volume was multiplied by 1.05 g/ml to obtain myocardial infarct mass. Total infarct mass was judged as non-assessable in four baseline scans, because the

region of delayed enhancement could not be differentiated clearly from the healthy myocardium in all myocardial segments (breathing artifacts, erroneous electrocardiographic triggering). These data were left out from the regression analysis.

Statistical analysis. All data are expressed as mean ± SD. Segmental data were stratified on baseline perfusion images in three groups: first, dysfunctional segments without MO; second, dysfunctional segments with MO; and third, remote myocardium. One-way analysis of variance was used for the comparison of EDWT measurements (at five days and at five months) between the three groups, followed by unpaired *t* tests. Two-way analysis of variance with repeated measures over time was used to compare changes in SWT between five days and five months and to evaluate the difference in these changes between the three groups. Bonferroni correction was applied to adjust for multiple comparisons. Univariate linear regression analysis was used to evaluate the relationship between infarct mass at five days and five months. Significance was accepted at $p \leq 0.05$.

RESULTS

Myocardial infarct size. Mean infarct size decreased significantly with 31%, from 35 ± 21 g at five days to 24 ± 17 g at five months ($p < 0.001$), which was 26 ± 14% to 20 ± 11% of LV mass. Infarct size decreased relatively to the same extent in small and large infarctions ($r = 0.92$; $p < 0.001$) (Fig. 1). Anterior infarctions decreased from a mean of 36 to 25 g (30% reduction), as much as inferolateral infarctions, which decreased from 33 to 22 g (33% reduction). Remote LV mass decreased slightly but not statistically significantly from 100 ± 26 g to 94 ± 23 g ($p = 0.18$).

LV wall characteristics. Dysfunctional segments without MO had an increased EDWT at five days compared with remote myocardium (9.2 ± 1.7 mm vs. 8.4 ± 1.7 mm; $p < 0.001$) and segments with MO, despite a stented and patent coronary artery (8.4 ± 1.7 mm; $p = 0.07$) (Fig. 2A). At five months, segments without MO had a reduced EDWT comparable to the thickness of remote segments (7.8 ± 1.6 mm vs. 7.6 ± 1.4 mm; $p = 0.60$) (Fig. 2B) and demonstrated improvement in SWT (21 ± 15% to 40 ± 24%; $p < 0.001$), although function remained impaired compared with remote myocardium (40 ± 24% vs. 71 ± 29%; $p < 0.001$) (Fig. 3). Segments with MO demonstrated wall thinning at five months compared with remote segments (6.4 ± 1.3 mm vs. 7.6 ± 1.4 mm; $p = 0.006$) and no significant recovery of SWT (12 ± 14% to 17 ± 20%; $p = 0.15$).

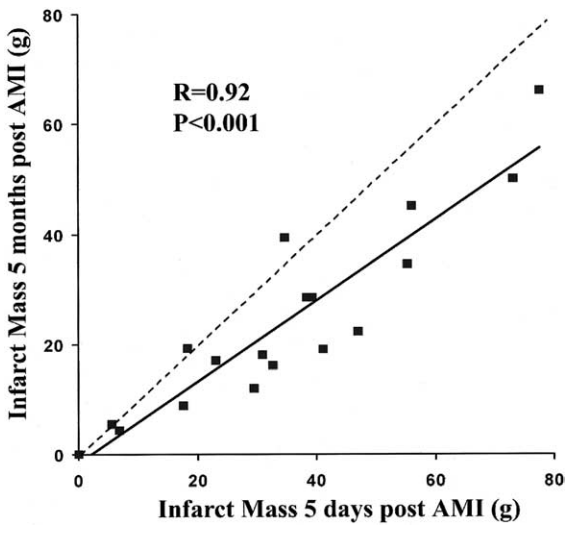

Figure 1. Relation between myocardial infarct mass at five days and five months after acute myocardial infarction (AMI) **(solid line)**. Equation: $y = 0.71x - 1.5$. **Dashed line** represents the line of unity (i.e., infarct mass at baseline is infarct mass at follow-up).

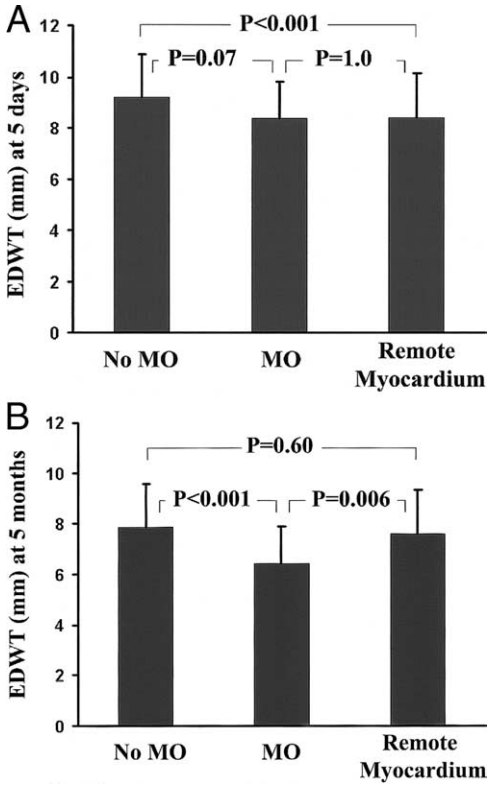

Figure 2. (A) Dysfunctional segments without microvascular obstruction (MO) had an increased end-diastolic wall thickness (EDWT) at five days compared with remote myocardium and myocardium with MO. **(B)** At five months, segments with MO demonstrated wall thinning compared with remote myocardium and myocardium without MO. End-diastolic wall thickness of myocardium without MO became comparable to remote myocardium.

DISCUSSION

In our study of 22 patients who underwent successful drug-eluting stent implantation within six hours of onset of symptoms, we first demonstrated that infarct size decreased relatively to the same extent in small and large infarctions, with a mean decrease of 31%. Second, we observed that dysfunctional segments without MO exhibited an increased EDWT compared with remote myocardium. These segments showed a significant improvement in wall thickening.

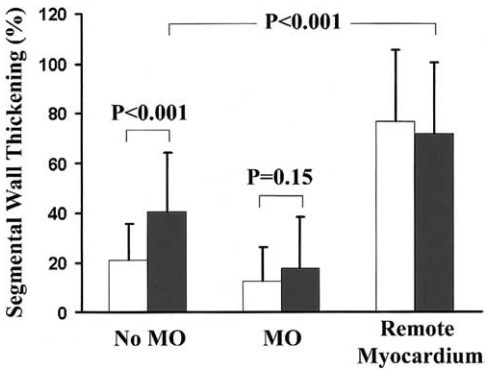

Figure 3. Dysfunctional myocardial segments without microvascular obstruction (MO) demonstrated improved segmental wall thickening at follow-up, but function remained impaired compared with remote myocardium. **Open bars** = five days; **solid bars** = five months.

Third, segments with MO, despite a stented coronary artery, demonstrated wall thinning at five months and showed no significant improvement in wall thickening at follow-up.

The pathophysiology of infarct healing and LV remodeling has been studied in a canine model of AMI (16). Infarct healing seemed to be an ongoing process, with early infarct expansion (four days) followed by infarct resorption, scar formation, and wall thinning (six weeks). Necrotic myocytes, interstitial edema, hemorrhage, and inflammatory cells were resorbed and replaced by collagenous scar tissue. Infarct healing might be further enhanced by repopulation of the border zones of the infarcted area by circulating stem cells (17). Remote myocardial mass increased in an animal study of AMI (3), whereas in our study, a small but nonsignificant reduction in remote myocardial mass was observed. This observation in our study might be explained by early and chronic treatment with angiotensin-converting enzyme inhibition in 18 patients (82%) and beta-blockers in 22 patients (100%).

Studying infarct size reduction in patients has recently become possible with the introduction of high-resolution ce-MRI. Contrast-enhanced MRI allows the differentiation of necrotic and viable myocardium with delayed-enhancement imaging, besides the assessment of myocardial wall thickening with cine-MRI and myocardial perfusion and MO with first-pass perfusion imaging (3,5,8,11,18,19). Therefore, ce-MRI is a suitable non-invasive imaging tool to evaluate the natural course of infarct healing and to evaluate stem-cell therapy for AMI. Promising but contradictory results have been reported (20–22). The nonrandomized Transplantation of Progenitor Cells and Regeneration Enhancement in Acute Myocardial Infarction (TOPCARE-AMI) trial studied acute infarct patients who were treated with coronary stenting with a mean time of reperfusion of 23 h, followed by coronary infusion of adult progenitor cells at four days. They demonstrated an increase in ejection fraction of 5% at 4 months and of 9% at 12 months. Infarct size decreased approximately 20% at 4 months and 34% at 12 months. In the randomized Bone Marrow Transfer to Enhance ST-Elevation Infarct Regeneration (BOOST) trial, patients were eligible for inclusion if admitted within five days of onset of symptoms. Ejection fraction increased by 7% in patients treated with bone-marrow cells and 1% in patients treated conventionally. Infarct size decreased in both patient groups by approximately 30% to 35% in six months. Ingkanisorn et al. (23) studied patients with acute or subacute (up to one month) revascularization therapy and observed an increase in ejection fraction of 5% and a decrease in infarct size of approximately 34% in five months. In the present study, patients were revascularized within six hours and received optimal pharmacological treatment for AMI. An improvement in ejection fraction of 7% was demonstrated, and infarct size decreased by 31% in five months. From these studies, it might be concluded that there seems to be no difference in decrease of infarct size (approximately 30% to 35%) between patients treated with mechanical perfusion alone or with the combination of infusion of either bone marrow or adult progenitor cells and mechanical reperfusion. The increase in ejection fraction ranged between approximately 5% and 7%, and only in the control group of the BOOST trial did the ejection fraction remain nearly unchanged. It remains to be seen whether infarct size or ejection fraction or the combination needs to be taken as the primary end point in the investigations of reperfusion strategies in AMI.

Restoration of epicardial coronary flow by primary angioplasty is highly successful in patients with AMI, and the occurrence of target vessel restenosis has been reduced dramatically since the introduction of drug-eluting stents (13); however, the effect of restoration of epicardial coronary blood flow on ischemic myocardium is not well understood. In a porcine model of AMI, restoration of myocardial perfusion was followed by an increase in EDWT presumed to be due to hyperemia and extravasation of fluids (24,25). Histology of reperfused segments with increased EDWT revealed massive extra-cellular edema but an intact microvasculature (24). We observed, in line with these experimental studies, that segments without MO demonstrated an increased EDWT; however, restoration of epicardial coronary blood flow is not always followed by restored microvascular perfusion. Microvascular obstruction might occur owing to obstructing microthrombi originating from the primary occluding thrombus, microvascular plugging by the influx of inflammatory cells, and/or locally emerging thrombi caused by endothelial damage by oxygen radicals (4,26). In our study, myocardial segments with MO did not demonstrate an increased EDWT. This was most likely caused by reduced blood-flow in myocardium with MO and subsequently less extravasation of fluids to the interstitium. Interestingly, these segments demonstrated wall-thinning at follow-up, and myocardial contractility remained severely depressed.

Reprint requests and correspondence: Dr. Pim J. de Feyter, Erasmus Medical Center, Department of Cardiology and Radiology, Thoraxcenter, Room Ba 591, Dr. Molewaterplein 40, 3000 GD Rotterdam, the Netherlands. E-mail: p.j.defeyter@erasmusmc.nl.

REFERENCES

1. Keeley EC, Boura JA, Grines CL. Primary angioplasty versus intravenous thrombolytic therapy for acute myocardial infarction: a quantitative review of 23 randomised trials. Lancet 2003;361:13–20.
2. Christian TF, Schwartz RS, Gibbons RJ. Determinants of infarct size in reperfusion therapy for acute myocardial infarction. Circulation 1992;86:81–90.
3. Fieno DS, Hillenbrand HB, Rehwald WG, et al. Infarct resorption, compensatory hypertrophy, and differing patterns of ventricular remodeling following myocardial infarctions of varying size. J Am Coll Cardiol 2004;43:2124–31.
4. Verma S, Fedak PW, Weisel RD, et al. Fundamentals of reperfusion injury for the clinical cardiologist. Circulation 2002;105:2332–6.
5. Gerber BL, Rochitte CE, Melin JA, et al. Microvascular obstruction and left ventricular remodeling early after acute myocardial infarction. Circulation 2000;101:2734–41.
6. Mahrholdt H, Wagner A, Holly TA, et al. Reproducibility of chronic infarct size measurement by contrast-enhanced magnetic resonance imaging. Circulation 2002;106:2322–7.
7. Yang Z, Berr SS, Gilson WD, Toufektsian MC, French BA. Simultaneous evaluation of infarct size and cardiac function in intact mice by contrast-enhanced cardiac magnetic resonance imaging reveals contractile dysfunction in noninfarcted regions early after myocardial infarction. Circulation 2004;109:1161–7.
8. Judd RM, Lugo-Olivieri CH, Arai M, et al. Physiological basis of myocardial contrast enhancement in fast magnetic resonance images of 2-day-old reperfused canine infarcts. Circulation 1995;92:1902–10.
9. Wu KC, Kim RJ, Bluemke DA, et al. Quantification and time course of microvascular obstruction by contrast-enhanced echocardiography and magnetic resonance imaging following acute myocardial infarction and reperfusion. J Am Coll Cardiol 1998;32:1756–64.
10. Amado LC, Kraitchman DL, Gerber BL, et al. Reduction of "no-reflow" phenomenon by intra-aortic balloon counterpulsation in a randomized magnetic resonance imaging experimental study. J Am Coll Cardiol 2004;43:1291–8.
11. Kim RJ, Fieno DS, Parrish TB, et al. Relationship of MRI delayed contrast enhancement to irreversible injury, infarct age, and contractile function. Circulation 1999;100:1992–2002.
12. Chesebro JH, Knatterud G, Roberts R, et al. Thrombolysis In Myocardial Infarction (TIMI) trial, phase I: a comparison between intravenous tissue plasminogen activator and intravenous streptokinase. Clinical findings through hospital discharge. Circulation 1987;76:142–54.
13. Lemos PA, Saia F, Hofma SH, et al. Short- and long-term clinical benefit of sirolimus-eluting stents compared to conventional bare stents for patients with acute myocardial infarction. J Am Coll Cardiol 2004;43:704–8.
14. Slavin GS, Wolff SD, Gupta SN, Foo TK. First-pass myocardial perfusion MR imaging with interleaved notched saturation: feasibility study. Radiology 2001;219:258–63.
15. Holman ER, Buller VG, de Roos A, et al. Detection and quantification of dysfunctional myocardium by magnetic resonance imaging. A new three-dimensional method for quantitative wall-thickening analysis. Circulation 1997;95:924–31.
16. Richard V, Murry CE, Reimer KA. Healing of myocardial infarcts in dogs. Effects of late reperfusion. Circulation 1995;92:1891–901.
17. Orlic D, Hill JM, Arai AE. Stem cells for myocardial regeneration. Circ Res 2002;91:1092–102.
18. Rehwald WG, Fieno DS, Chen EL, Kim RJ, Judd RM. Myocardial magnetic resonance imaging contrast agent concentrations after reversible and irreversible ischemic injury. Circulation 2002;105:224–9.
19. Baks T, van Geuns RJ, Biagini E, et al. Recovery of left ventricular function after primary angioplasty for acute myocardial infarction. Eur Heart J 2005;26:1070–7.
20. Britten MB, Abolmaali ND, Assmus B, et al. Infarct remodeling after intracoronary progenitor cell treatment in patients with acute myocardial infarction (TOPCARE-AMI): mechanistic insights from serial contrast-enhanced magnetic resonance imaging. Circulation 2003;108:2212–8.
21. Schachinger V, Assmus B, Britten MB, et al. Transplantation of progenitor cells and regeneration enhancement in acute myocardial infarction: final one-year results of the TOPCARE-AMI trial. J Am Coll Cardiol 2004;44:1690–9.
22. Wollert KC, Meyer GP, Lotz J, et al. Intracoronary autologous bone-marrow cell transfer after myocardial infarction: the BOOST randomised controlled clinical trial. Lancet 2004;364:141–8.
23. Ingkanisorn WP, Rhoads KL, Aletras AH, Kellman P, Arai AE. Gadolinium delayed enhancement cardiovascular magnetic resonance correlates with clinical measures of myocardial infarction. J Am Coll Cardiol 2004;43:2253–9.
24. Turschner O, D'Hooge J, Dommke C, et al. The sequential changes in myocardial thickness and thickening which occur during acute transmural infarction, infarct reperfusion and the resultant expression of reperfusion injury. Eur Heart J 2004;25:794–803.
25. Pislaru C, Bruce CJ, Seward JB, Greenleaf JF. Distinctive changes in end-diastolic wall thickness and postsystolic thickening in viable and infarcted myocardium. J Am Soc Echocardiogr 2004;17:855–62.
26. Kloner RA, Ganote CE, Jennings RB. The "no-reflow" phenomenon after temporary coronary occlusion in the dog. J Clin Invest 1974;54:1496–508.